High-Resolution Planar Two-Component PTV Measurements in a Breaking Wave

Malene H. Vested[1,*], F. Gökhan Ergin[2], Stefan Carstensen[1], Erik D. Christensen[1]

1: Section of Fluid Mechanics, Coastal and Maritime Engineering, Dep. of Mech. Eng., Technical University of Denmark, Denmark

2: Microfluidics Product Manager, Dantec Dynamics, Denmark

* Correspondent author: mlhv@mek.dtu.dk

Keywords: PTV, Dynamic Masking, Two-Phase flow, Interface, Ocean waves, Wave forces

ABSTRACT

Ocean waves and the associated wave forces are of vital importance for marine applications, with offshore wind turbines as one example. Since the wave forces are governed by the wave kinematics, detailed studies of wave kinematics are highly valuable. In this study, wave kinematics of a breaking laboratory wave is investigated using dynamic masking and Particle Tracking Velocimetry (PTV). First, dynamic masking is used to remove the bubble-droplet layer above the free surface. Second, PTV is used to resolve the kinematics with high spatial resolution throughout the wave motion from the laboratory bed to the water surface. Instantaneous velocity fields are obtained at a sample rate of 96Hz, and this provides sufficient temporal resolution for spectrum and acceleration investigations. The results indicate that, compared to Particle Image Velocimetry (PIV), the current methodology provides a better understanding for the dynamics of ocean waves, thus leading to more accurate predictions of wave forces.

1. Introduction

The study of ocean waves is essential to multiple marine applications, including offshore wind turbines. Offshore wind energy is an expanding industry with wind turbines now planned and installed at greater water depths. In order to ensure a low cost of the wind turbine without compromising structural reliability, the wave forces acting on the foundation must be accurately predicted. When predicting the dynamic wave forces, it is vital to know the wave kinematics, that is, velocities as well as accelerations. To this end, laboratory measurements of water waves at high spatial and temporal resolution are very important. Measurements of water waves in the laboratory, however, represent a number of challenges since it is a two-phase flow with a moving interface. For wake kinematics investigations, both PIV and PTV are well suited, while PTV provides a better spatial resolution.

Water waves, including breaking events, have already been studied through PIV measurements by Perli, He & Bernal (1996), Grue et al. (2003), Kimmoun, Branger & Zucchini (2004), Belden & Techet (2011), André & Bardet (2014) among others. One common challenge for PIV investigations for breaking waves is the contribution of the bubble-droplet layer at the air-water interface in the cross-correlation function. This is a general problem for PIV in two-phase flows. This is because the cross-correlation-based PIV algorithms can not distiguish between the two phases, and often, cross-talk exists close to the phase-boundary due to the finite size of the PIV interrogation window, Ergin (2017). Ironically, important fluid mechanics phenomena takes place at the phase boundary. One way of addressing this challenge is to mask out the phase that is not of interest.

Dynamic masking techniques have the advantage of automatically masking the unwanted phase from the PIV images, which is convenient for large datasets. The flow around a single bubble rising in a water column was studied by Hassan, Ortiz-Villafuerte & Schmidl (2001), in which the interface between the bubble and the flow was masked by an edge-tracking technique. Another edge-tracking technique was suggested by Guo et al. (2010) to extract bubbles from a flow field. In a recent study by Dussol et al. (2016), an image masking process is used to investigate the flow field close to a vessel by using a predefined shape of the vessel. Sanchis & Jensen (2011) suggest a Radon-transform method to detect the interphase between air and water in a PIV measurement of an overturning wave. The Radon-transform method detects smaller sections of straight lines and captures the particles on the free surface. Subsequently, the smaller sections are fitted to a polynomial to obtain the free surface. This method, however, is less succesful in the case of breaking waves where the shape is not well represented by a polynomial or any other pre-defined function. A comprehensive list of dynamic masking references is provided by Ergin (2017).

In this work, a histogram-thresholding-based dynamic masking procedure is applied (Ergin 2017). Furthermore, we have used a hybrid PIV/PTV technique to obtain the time-resolved flow field information. The combination of PIV and PTV offers a high spatial resolution, since it combines the robustness of PIV with the high spatial resolution of PTV, Keane, Adrian & Zhang (1995), Stotou & Riethmuller (2001). Furthermore, PTV has been found to increase accuracy close to boundaries (Kähler, Scharnowski, and Cierpka 2012).

The objective of this work is to obtain accurate and high resolution – both in time and in space – velocity measurements in a typical ocean wave. The aim is to compute accelerations from the time-resolved velocity data. Accurate studies of the wave kinematics ultimately leads to better wave force estimates, which can be used in the production of reliable and low cost offshore wind turbines.

The paper is structured as follows: The experimental setup is explained in section 2, with a description of the PTV setup as well as the laboratory flume. In section 3 the image pre-processing is presented followed by the application of a dynamic masking procedure and in section 4 we show how detailed velocity information is obtained by the use of PIV / PTV. In section 5 we discuss on a spectrum analysis of the velocity and the associated acceleration field computed from the velocity information is presented. Section 6 concludes on the results from the study.

2. Experimental set-up

The experiment was conducted in a wave-current flume at the Hydraulic Laboratory of the Technical University of Denmark (Fig. 1). It has a length of 28.0m -, width of 0.60m - and a depth of 0.80m. Waves are generated by a piston-type wave paddle positioned at one end of the flume at a water depth of 0.515m. In order to investigate steep and breaking waves, an inclined, smooth seabed of slope 1/25 is installed in the wave flume. As the waves travel from the wave generator and up the seabed, the waves steepen and wave breaking occurs at a certain water depth. Here, we have investigated a wave that breaks at a distance of 19.8m from the wave paddle with a breaking wave height of 0.17 m and wave period of 1.5s . The water surface elevation is measured at 6 locations in the flume with resistance wave gauges.

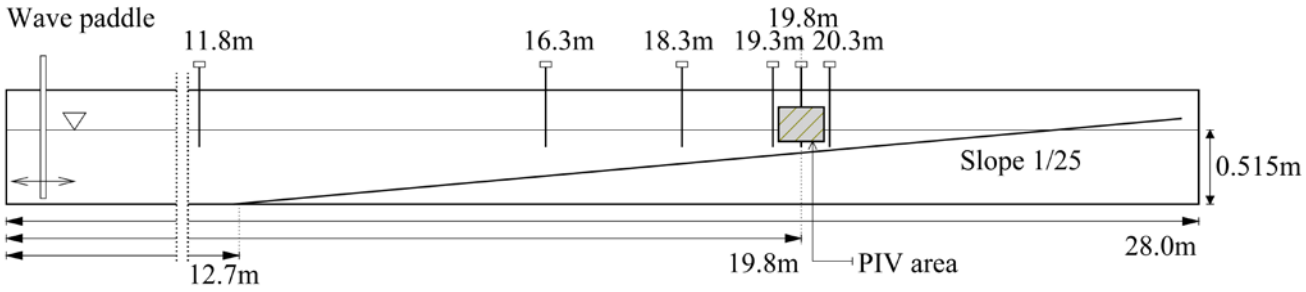

Fig. 1 Schematic of the wave-current flume with the wave paddle to the left. The waves travel on a flat bed for 12.7m before travelling onto a 1/25 slope, which causes the waves to steepen and ultimately break.

The PIV / PTV measurement system is manufactured by Dantec Dynamics. Fig. 2a shows a cross-sectional sketch of the flume and the PIV / PTV measurement setup. The sidewall of the wave flume is made from glass, and furthermore a glass window is incorporated into the inclined laboratory bed. Upon reflection from a 45° tilted mirror placed below the inclined bed, the light sheet illuminates the measurement area vertically from below. The high-frequency PIV laser

(DualPower 100-100) is a dual-cavity, ND:YAG laser emitting 532nm light. Each cavity can produce 100mJ pulse energy at a rate of 100Hz with a pulse length of 12ns. The thickness of the laser sheet ranges from 2 mm to 2.8 mm in the measurement area. The particle images are captured

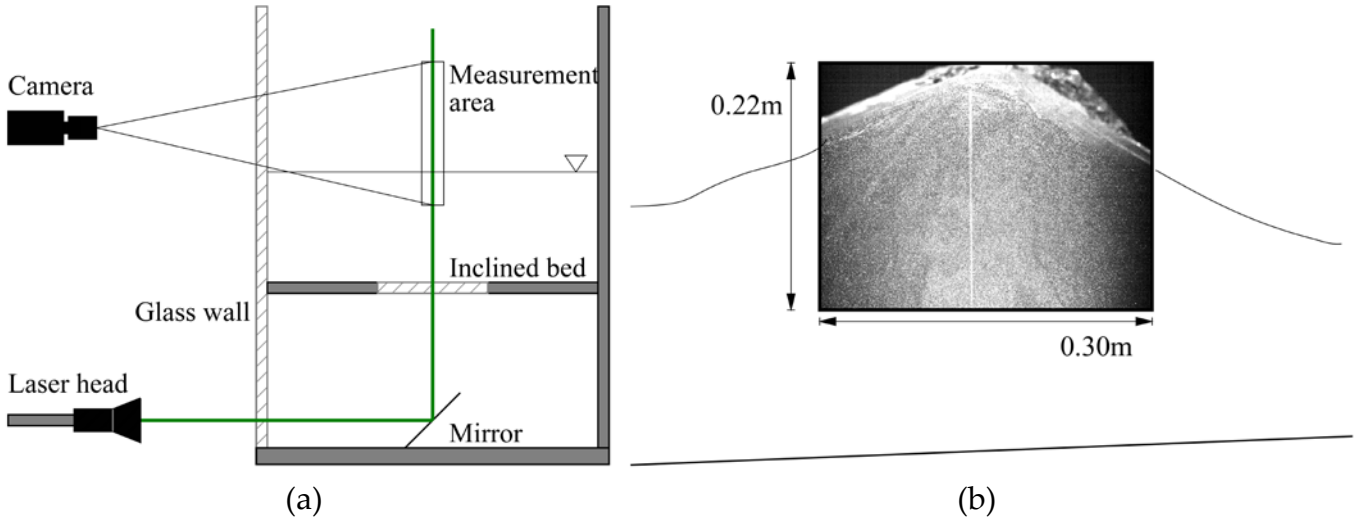

Fig. 2 (a) Cross-sectional view of the wave flume at the PIV / PTV measurement area. The horizontal laser sheet reflects on a 45°-tilted mirror at the bottom of the wave flume and propagates vertically through a window in the inclined, smooth laboratory bed. (b) Field of view of the PIV / PTV measurement area.

using a 4Mpix, SpeedSense1040 4MP camera with a 50mm lens and the pixel resolution is 2320×1726 pixels. The flow is seeded with silver-coated hollow glass spheres with a buoyancy of 1 g/cc and a mean diameter of 10 μm. The seeding particles ensure a high reflection thanks to the silver coating. Double-images are sampled at 96 Hz with an interframe time of 5ms. The PIV / PTV measurement area covers 0.30×0.22 m and the water depth at the measurement location is 205mm. Fig. 2b shows the field-of-view of the PIV / PTV measurement area, with a snapshot of the raw image inserted.

3. Image Pre-processing and Dynamic Masking

During image pre-processing, the following image pre-processing steps were performed; background subtraction, application of a Gaussian difference filter and a histogram-threshold based dynamic masking. Before the velocity calculation, it was necessary to perform image pre-processing on the raw particle images. The particle image is shown in Fig. 3, which depicts the wave as it is overturning. Note that the vertical line thought the center of the image is the wave gauge measuring the surface elevation. First, a background image pair was computed based on

the temporal minimum pixel value of all the aquired raw images. The background image was then subtracted from the raw images in the ensemble. In Fig. 4a the inverted particle image is shown after the background subtraction. Subsequently, the particle images were enhanced using a

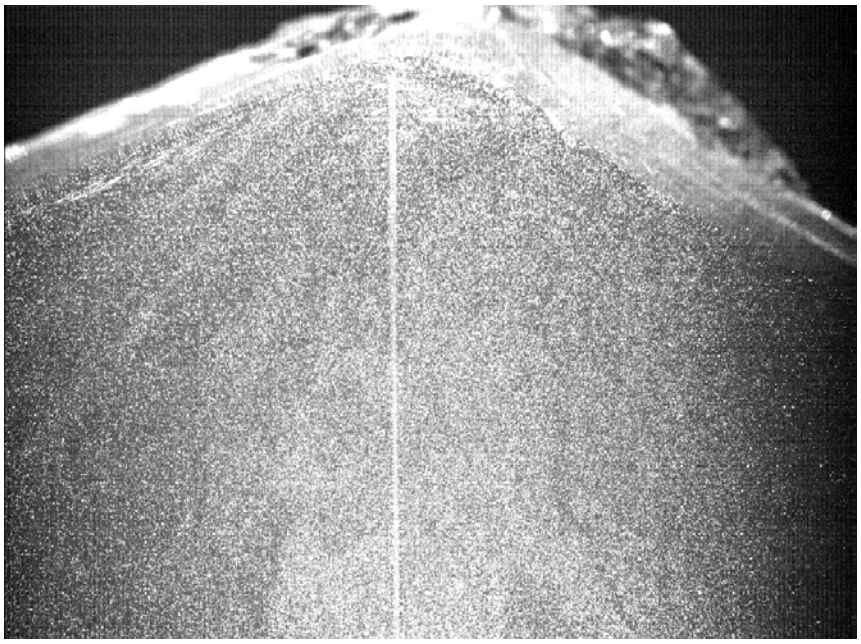

Fig. 3 Particle image at t=0.646s. The vertical line seen in the center is a wave gauge.

difference of Gaussian (DoG) filter (Ergin et al. 2014). Briefly, the DoG filter is the difference between an image filtered by 7×7 Gaussian filter and the same image filtered by a 3×3 Gaussian filter. The resulting particle image, shown in Fig 4b, is filtered from noise caused by the background disturbance, wave gauge and the air-water mixture above the water surface during the breaking event. The last step before the actual dynamic masking is the application of a sequence of opening and closing filters, in this case a combination of 10 opening filters followed by 15 closing filters (Fig. 4c). As a final step, a histogram-treshold based dynamic masking is applied on the DoG filtered images in order to clean out intermittent laser reflections and a few bright pixels above the water surface in Fig. 4b.

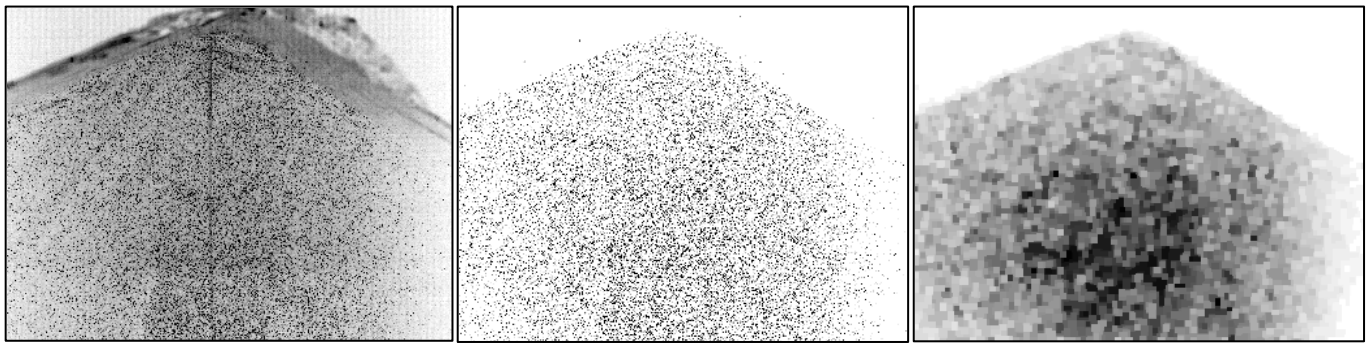

(a) (b) (c)

Fig. 4 (a) Inverted raw particle image after background subtraction. (b) After application of Difference of Gaussian filter (c) Pre-processed image used for histogram-threshold based dynamic masking. All at t=0.646s.

4. PIV / PTV Results

After the dynamic masking process, the velocities are computed through a three-step procedure. First, a preliminary Particle Image Velocimetry (PIV) analysis is performed, see Fig. 5a. The PIV algorithm is an adaptive PIV with an initial interrogation area of 64x64 pixel and final interrogation area of 32×32, using a grid step size of 16×16 pixels (50% overlap). The interrogation area size was adapted to the particle density with a minimum of five particles as the limit. A universal outlier detection (UOD) was applied and outliers were substituted by the local median. The PIV result is used as input for the subsequent PTV analysis. Second, the PTV was computed through a 2-pass particle-matching scheme. A total of 28,697 particles were matched at the time instant where the wave is at its highest point. A separate new UOD scheme was used after the PTV analysis. The velocity field computed by PIV and PTV are shown in Fig. 5a and 5b, respectively. Comparing these subfigures we notice that many of the spurious vectors calculated close to the free surface are eliminated using the PTV technique. Furthermore, some of the velocity vectors smoothened during the PIV analysis were re-captured in the PTV analysis. (Observe e.g. one red velocity vector in a zone of yellow velocity vectors in Fig. 5b in the middle to the left). Finally, the PTV results are interpolated back onto a Cartesian grid using a spline interpolation scheme (Fig. 6) in order to perform subsequent vector post processing.

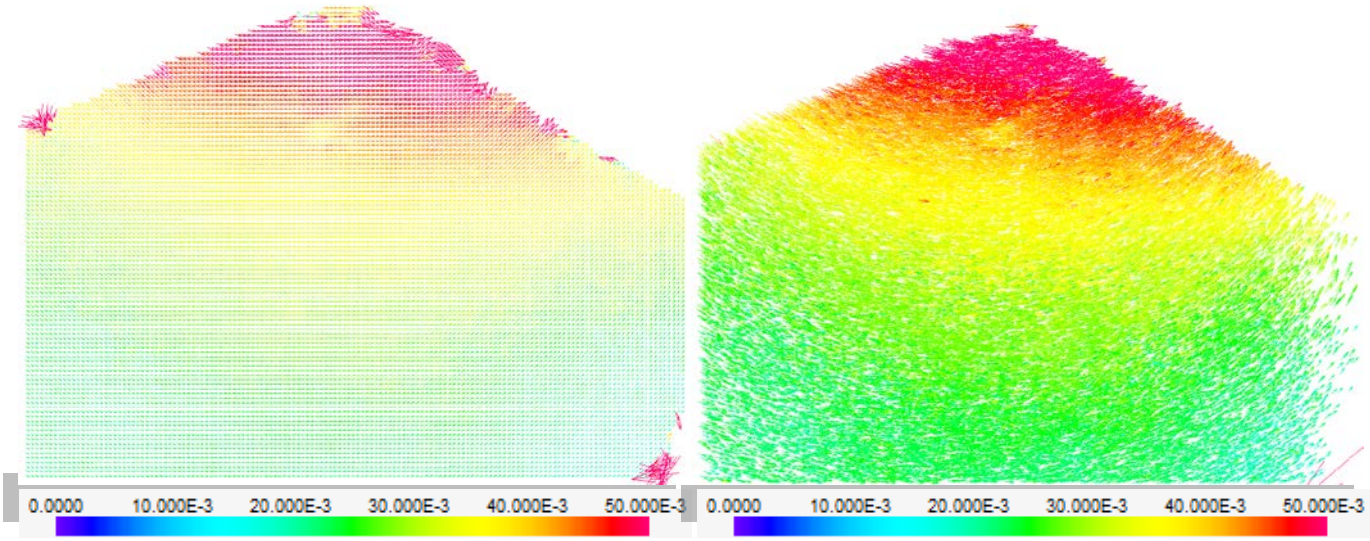

(a) (b)

Fig. 5 (a) Preliminary PIV analysis used as input for subsequent PTV analysis. Color bar is velocity [m/s] (b) PTV results. Color bar is velocity [m/s]. Both at t=0.646s.

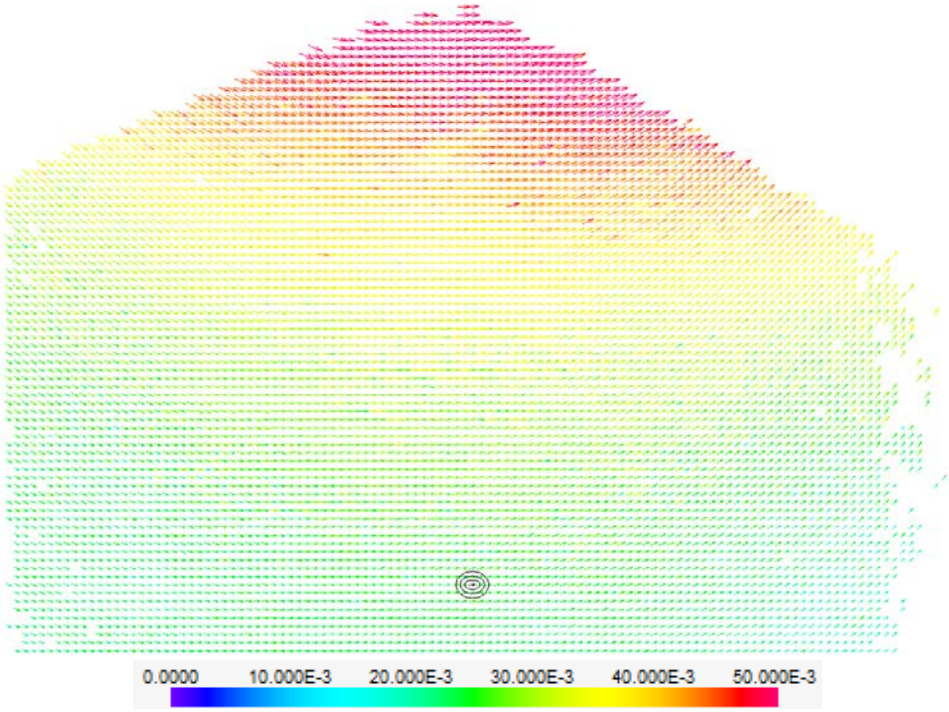

Fig. 6 PTV-result interpolated back onto Cartesian grid at t=0.646s. Color bar is velocity [m/s]

The PTV analysis serves three purposes here: Firstly, it acts as an outlier detector for the PIV result. In particular, the spurious vectors in the areas close to the water surface and in the less-illuminated corners are removed (Fig. 5a). Secondly, the spatial resolution is improved compared to PIV, since

the spatial smoothing is reduced. Thirdly, the accuracy of the computed velocity is improved, since PTV allows for greater local variation of velocity, due to the reduced smoothing. Thus, applying PTV provides improved results for wave kinematics throughout the flow field.

4. Spectrum and acceleration measurements

Once the PTV results with high spatial and temporal resolution are obtained, further post-processing steps such as spectrum and acceleration calculations can be performed. First, the velocity time series, u(t) and v(t), at a single point, indiacted by the black circle in Fig. 6, are shown in Fig. 7. Comparing the horizontal and vertical velocity time series, it is seen that the horizontal velocity displays a larger amplitude with peak velocity 70% larger than peak amplitude of the verticxal velocity. It is seen that the horizontal velocity increases rapidly as the wave approaches breaking around t=0.65s, while the vertical velocity peaks just before breaking around t=0.5s. A small-amplitude fluctuation can be observed in the v(t) which is not seen for u(t).

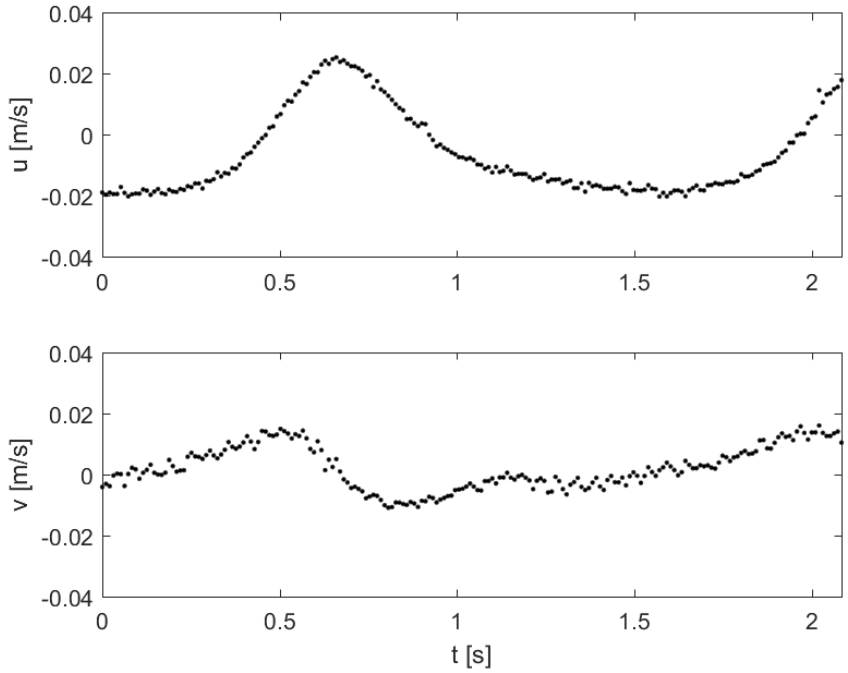

Fig. 7 Velocity time series in the horizontal, u(t), and in the vertical, v(t), obtained at the black circle in Fig. 6.

A spectrum analyis of the velocities is presented in Fig. 8. The spectrum of v(t) indicates that the measured fluctuation frequency is at 19.2 Hz (Fig. 8). At this point, the reason for this fluctuation is not clear, and this will be the subject of future investigations.

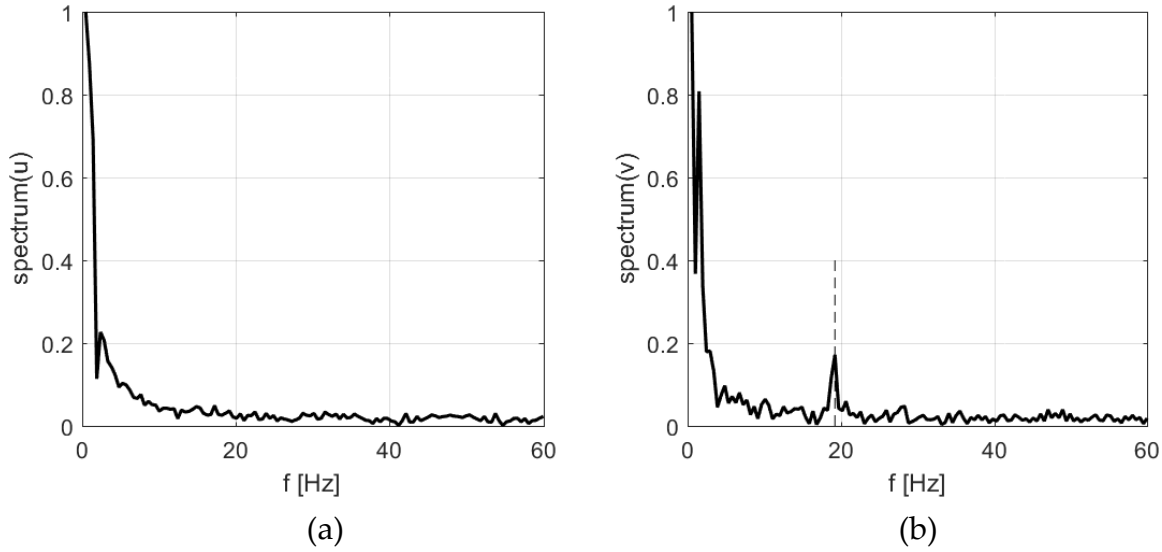

(a) (b)

Fig. 8 Spectrum analysis, (a) horizontal velocity u(t), (b) vertical velocity v(t).

Second, the acceleration is computed by a right-sided first order finite difference scheme: $\frac{du}{dt}_i \cong \frac{u_{i+1}-u_i}{\Delta t}$, and the acceleration field at t=0.646s is shown in Fig. 9. The acceleration results indicate that the rightwards-propogating wave has rightward acceleration on the right and leftward acceleration on the left. This is expected due to the breaking occuring around this time instant.

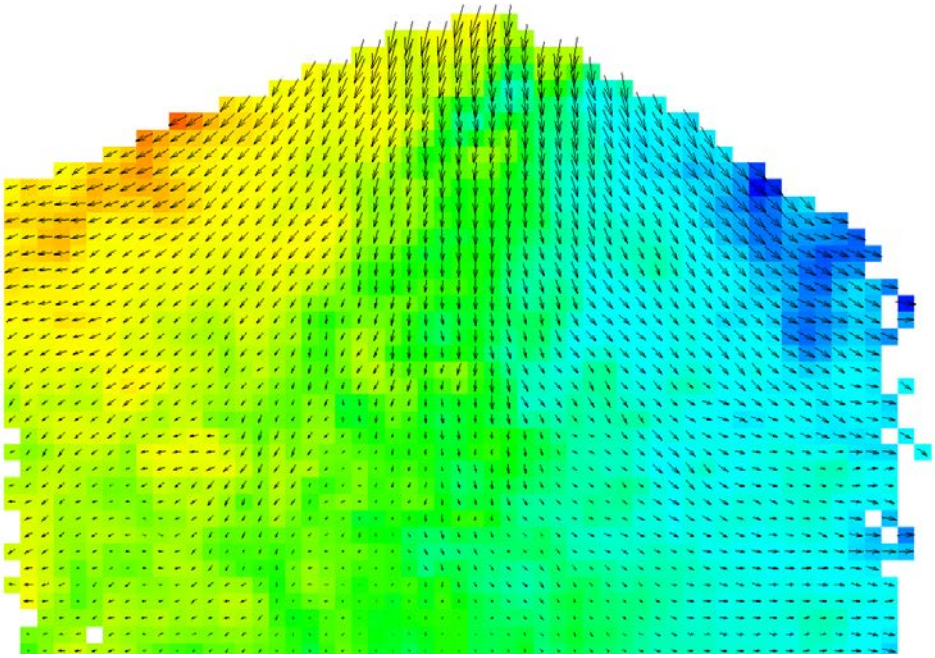

Fig. 9 Acceleration field at t=0.646s. Vectors represent the total acceleration magnitude and direction, where colors represent acceleration only in the horizontal direction (warmer colors towards left and colder colors toward right).

5. Conclusions

We present here a high-resolution PTV study of a breaking wave. We have demonstrated that careful image pre-processing and histogram-thresholding based dynamic masking is successful in masking the air phase and the bubble-droplet mixture on the free surface and therefore very suitable in wave kinematics investigations. Furthermore, we found that the applied PTV algorithm improves the data in three points: 1) The PTV algorithm acts as an outlier detector for PIV, 2) PTV provides improved spatial resolution compared to PIV, due to the reduced spatial smoothing and 3) PTV provides more accurate velocities. The velocity information obtained from PTV was succesfully used to compute the associated acceleration field. The detailed kinematics uncovered by these measurements are of great importance in marine applications including the offshore wind energy industry, for which wave dynamics and wave forces on the substructures play an essential role. Future work will include force estimates based on the obtained kinematics for wave loads on a monopile.

Acknowledgements

The study was partly supported by the DeRisk project funded by Innovation Fund Denmark, grant number 4106-00038B and partly by DHI.

References

André, Matthieu A. and Philippe M. Bardet. 2014. "Velocity Field, Surface Profile and Curvature Resolution of Steep and Short Free-Surface Waves." *Experiments in Fluids* 55(4).

Belden, Jesse and Alexandra H. Techet. 2011. "Simultaneous Quantitative Flow Measurement Using PIV on Both Sides of the Air-Water Interface for Breaking Waves." *Experiments in Fluids* 50(1):149–61.

Dussol, David, Philippe Druault, Bachar Mallat, Sylvain Delacroix, and Grégory Germain. 2016. "Automatic Dynamic Mask Extraction for PIV Images Containing an Unsteady Interface, Bubbles, and a Moving Structure." *Comptes Rendus - Mecanique* 344(7):464–78. Retrieved (http://dx.doi.org/10.1016/j.crme.2016.03.005).

Ergin, F. G., B. B. Watz, K. Erglis, and A. Cebers. 2014. "Modal Analysis of Magnetic Microconvection." *Magnetohydrodynamics* 50(4):339–52.

Ergin, F. Gökhan. 2017. "Dynamic Masking Techniques for Particle Image Velocimetry." *Isi Bilimi Ve Teknigi Dergisi/ Journal of Thermal Science and Technology* 37(2):61–74.

Grue, John, Didier Clamond, Morten Huseby, and Atle Jensen. 2003. "Kinematics of Extreme Waves in Deep Water." *Applied Ocean Research* 25(6):355–66.

Guo, Fude, Yahui Yang, Bin Chen, and Liejin Guo. 2010. "A Novel Multi-Scale Edge Detection Technique Based on Wavelet Analysis with Application in Multiphase Flows." *Powder Technology* 202(1–3):171–77. Retrieved (http://dx.doi.org/10.1016/j.powtec.2010.04.035).

Hassan, Yassin a., Javier Ortiz-Villafuerte, and William D. Schmidl. 2001. "Three-Dimensional Measurements of Single Bubble Dynamics in a Small Diameter Pipe Using Stereoscopic

Particle Image Velocimetry." *International Journal of Multiphase Flow* 27(5):817–42. Retrieved (http://linkinghub.elsevier.com/retrieve/pii/S0301932200000549).

Kähler, Christian J., Sven Scharnowski, and Christian Cierpka. 2012. "On the Uncertainty of Digital PIV and PTV near Walls." *Experiments in Fluids* 52(6):1641–56.

Keane, R. D., R. J. Adrian, and Y. Zhang. 1995. "Super-Resolution Particle Imaging Velocimetry." *Experiments in Fluids* 6:754–68.

Kimmoun, O., H. Branger, and B. Zucchini. 2004. "Laboratory PIV Measurements of Wave Breaking on Beach." *Isope* 14:293–98.

Perlin, Marc, Jianhui He, and Luis P. Bernal. 1996. "An Experimental Study of Deep Water Plunging Breakers." *Physics of Fluids* 8(9):2365–74.

Sanchis, Arnaud and Atle Jensen. 2011. "Dynamic Masking of PIV Images Using the Radon Transform in Free Surface Flows." *Experiments in Fluids* 51(4):871–80.

Stitou, Adel and M. L. Riethmuller. 2001. "Extension of PIV to Super Resolution Using Adel Stitou and M L Riethmuller." *Measurement Science and Technology* 12(12):1398–1403. Retrieved (http://iopscience.iop.org/0957-0233/12/9/304).